JCAMECH

Vol. 51, No. 1, June 2020, pp 55-65
DOI: 10.22059/jcamech.2020.290187.435

Pareto Optimal Balancing of Four-bar Mechanisms Using Multi-Objective Differential Evolution Algorithm

Ghazal Etesami[a], Mohammad Ebrahim Felezi[a,] ∗ and Nader Nariman-Zadeh [a]

[a] *Department of Mechanical Engineering, University of Guilan, Rasht, Iran*

ARTICLE INFO

Article history:
Received: 5 October 2019
Accepted: 17 January 2020

Keywords:
Multi-objective Optimization
Balancing
Four-bar Mechanism
Differential Evolution Algorithm
Pareto

ABSTRACT

Four-bar mechanisms are widely used in the industry especially in rotary engines. These mechanisms are usually applied for attaining a special motion duty like path generation; their high speeds in the industry cause an unbalancing problem. Hence, dynamic balancing is essential for their greater efficiency. In this research study, a multi-objective differential evolution algorithm is used for Pareto optimization balancing of a four-bar planar mechanism while considering the shaking moment and horizontal and vertical shaking forces as objective functions. This is necessary since the high magnitude of shaking forces and moment affect the fatigue life of the mechanism. The design variables are both kinematic and dynamic parameters of the moving links. The Pareto charts of five-objective optimization exhibit a large number of non-dominated points, which provide more choices for optimal balancing design of the planar four-bar mechanism. A comparison of the results obtained from this study with those reported in the literature shows a significant decrease in shaking forces and shaking moment.

1. Introduction

In the field of mechanism balancing, all studies aim to achieve the lowest shaking force and moment fluctuations so that the mechanism's fatigue life can be improved. Therefore, there have been several research studies on mechanism balancing reported in the literature during the last few decades. Researchers have used classical methods or old and new optimal approaches to achieve this goal. Moreover, optimization is one of the most important design issues in science, especially engineering [1-3]. In multi-objective optimization problems, several different objective functions are defined with the goal of simultaneous minimization or maximization [4-7]. This is the main difference between the general nature of single-objective and multi-objective problems. These objectives are often in conflict with each other. In other words, when one objective function improves, another one worsens .Therefore, there is no single optimal solution concerning all the objective functions. Usually in such problems, there exists a set of solutions that are equally good, well-known as Pareto optimal charts.

The concept of "Pareto" is named after a famous Italian economist called V. Pareto, who first found the theory of optimization with several objective functions in economy [8]. Pareto's theory or optimal set of solutions is the space of objective functions in multi-objective problems based on a set of solutions, none of which is superior to the others. In other words, changing the vector of design variables in the Pareto curve cannot result in improvement of all objective functions simultaneously due to resulting in deterioration of at least one objective function. It should be noted that these non-superior solutions are arranged in different layers based on the Pareto curve, which contain the most valuable solutions.

In the past few years, a novel algorithm called Differential Evolution (DE) has been presented as a profound and expeditious approach to optimize problems in continuous spaces. It is known as a new search approach and it has been initially introduced by Rainer Storn and Kenneth Price in 1995 [9, 10]. Both researchers proved that this algorithm exhibits exceptional competency in optimizing non-differentiable nonlinear functions [11]. The applied optimization algorithm of the present paper was also utilized in previous studies for kinematic optimization of mechanisms, and it has been rarely used in dynamic studies. Etesami et al. [12] used this algorithm in multi-objective dynamic balancing of a slider-crank mechanism. Qiao et al.[13] used a differential evolution algorithm for optimum kinematic design of spatial four-bar mechanism. An optimum synthesis of a four-bar mechanism by coupler control was performed using the differential evolution algorithm by Bulatovic et al.[14]. Lin et al.[15] proposed a new differential evolution algorithm with a combined mutation strategy for optimum synthesis of a path generating four-bar mechanism. Villarreal et al. [16] designed a five-bar parallel robot by a differential evolution algorithm. Shiacolus et al.[17] proposed an optimum synthesis of a six-bar mechanism using the differential evolution algorithm. Feng [18]

* Corresponding author. Tel.: +989111318827; e-mail: mefelezi@guilan.ac.IR

introduced a method to complete the moment balancing and shaking forces of eight-bar mechanisms via revolute joints. Furthermore, Ye and Smith [19] attained complete moment balancing via geared inertia counterweights. Li [20] presented shaking force and moment sensitivity formulation for planar articulating mechanisms. The robust balancing approach and sensitivity analysis, sensitive to fabrication processing errors are also presented. The objective function consisted of shaking moment and shaking force. The weighting factor values were chosen as equivalents. Arakelian et al.[21, 22] provided a solution to resolve the shaking moment and shaking force balancing of spatial and planar mechanisms. Arakelian [23] used the pantograph mechanism copying characteristics and the dynamic distributed masses replacement method via concentrated point masses to formulate circumstances for shaking moment and force balancing. Lowen and Tepper [24] applied counterweights to address a full force balance of planar linkages. Bahai and Esat [25] employed a full force and moment balanced approach by implementing geared counter-inertias for full force balanceable mechanism by the criteria of Tepper and Lowen's method.

Erkaya [26] used a genetic algorithm to optimize design variables to reduce shaking moment and forces and three weight coefficients for combining shaking moment and forces as the objective function. In previous studies, weight coefficients were used to combine objective functions and convert them into a single objective function. Selecting appropriate weight factors to combine the objectives functions is a difficult task. On the other hand, this act depends entirely on the selection of the designer. However, instead of three single-objective optimizations and obtaining three optimal points, one optimization is performed in this research study and as the Pareto charts show, many optimal points have been suggested to the designer. And the designer can select each one according to the design criteria and the designer is not limited in design point selection. In Reference [12] only dynamic balancing of the crank-slider mechanism has been performed and optimal mechanisms have been compared only with the main mechanism and its optimization results have not been compared with any other references. Therefore, superiority of the method used in ref [12] to methods proposed in other references has not been established while there is a comparison with previous research studies in the present study. However, the objective of the present study is using an evolutionary DE algorithm to optimize the multi-objective dynamic balancing of a planar four-bar mechanism, where the designer is not required to choose the weight coefficients for combining the objective functions.

The Differential Evolution (DE) Algorithm is a population-based, combinatorial algorithm and is able to find the global minimum of non-differentiable, discontinuous and non-linear functions similar to the GA. Experimental results have shown that the DE algorithm has advantages over GA. Moreover, it can effectively improve convergence speed and optimal quality. Hence, it shows excellent characteristics in the optimal design of systems like mechanisms and machines [27]. Therefore, it is a good choice to solve the optimization problem at hand.

In this case, the DE algorithm was used to obtain the most appropriate values of length, mass, moment of inertia and location of center of mass of the moving links of the planar mechanism as design variables and minimized shaking forces and moments as objective-functions. Five-objective functions included shaking moment, and the vertical and horizontal shaking forces simultaneously exerted on the frame of the mechanism. The Pareto charts were presented as a dyadic combination of objective functions. Finally, vibration performance of such design points were shown in comparison with other studies during a complete circling of input link [26]. Comparing the results with previous studies confirms the superiority of the method presented in the present research study.

2. Kinematic and dynamic formulation of four-bar mechanism

To investigate the effects of shaking force and shaking moment exerted in the frame, a four-bar planar mechanism was used in the balancing problems. The force diagram of the mechanism is shown in Figure.1. Kinematic analysis of the mechanism's model consists of determining displacements, velocities, and accelerations of moving links. Mass center positions of the moving links relative to the crank pivot are provided in the following form [26]:

$$\begin{bmatrix} x_{G2} \\ Y_{G2} \end{bmatrix} = r_2 \begin{bmatrix} \cos(\theta_2 + \alpha_2) \\ \sin(\theta_2 + \alpha_2) \end{bmatrix} \tag{1}$$

$$\begin{bmatrix} x_{G3} \\ Y_{G3} \end{bmatrix} = L_2 \begin{bmatrix} \cos\theta_2 \\ \sin\theta_2 \end{bmatrix} + r_3 \begin{bmatrix} \cos(\theta_3 + \alpha_3) \\ \sin(\theta_3 + \alpha_3) \end{bmatrix} \tag{2}$$

$$\begin{bmatrix} x_{G4} \\ Y_{G4} \end{bmatrix} = L_1 \begin{bmatrix} \cos\theta_1 \\ \sin\theta_1 \end{bmatrix} + r_4 \begin{bmatrix} \cos(\theta_4 + \alpha_4) \\ \sin(\theta_4 + \alpha_4) \end{bmatrix} \tag{3}$$

Where $x_{Gi}$and y_{Gi} for i =2, 3, 4 are the displacements at the x and y directions for mass center of the ith moving link; considering the input link, follower and coupler, correspondingly. Also, θ_2, θ_3 and θ_4 represent the angular positions of input, coupler and follower links relative to the x-direction, correspondingly (see appendix).Velocities and accelerations of mass centers can also be defined as time-derivatives of equations (1-3). α_2, $\alpha_3$and α_4 are named structural angles, and r_2, r_3 and r_4 are named structural links. In fact, α_i, r_i for i=2,3,4 are the angles and lengths made by connecting the center of mass to the beginning of each mechanism link.

Forces and moments were obtained by solving the systems of equilibrium equations of the mechanism:

$$\begin{bmatrix} -1 & 0 & 1 & 0 & 0 & 0 & 0 & 0 & 0 \\ 0 & -1 & 0 & 1 & 0 & 0 & 0 & 0 & 0 \\ r_{2y} & -r_{2x} & -r'_{2y} & r'_{2x} & 0 & 0 & 0 & 0 & 1 \\ 0 & 0 & -1 & 0 & 1 & 0 & 0 & 0 & 0 \\ 0 & 0 & 0 & -1 & 0 & 1 & 0 & 0 & 0 \\ 0 & 0 & r_{3y} & -r_{3x} & -r'_{3y} & r'_{3x} & 0 & 0 & 0 \\ 0 & 0 & 0 & 0 & -1 & 0 & 1 & 0 & 0 \\ 0 & 0 & 0 & 0 & 0 & -1 & 0 & 1 & 0 \\ 0 & 0 & 0 & 0 & r'_{4y} & -r'_{4x} & -r_{4y} & r_{4x} & 0 \end{bmatrix} \times \begin{bmatrix} F_{21x} \\ F_{21y} \\ F_{32x} \\ F_{32y} \\ F_{43x} \\ F_{43y} \\ F_{41x} \\ F_{41y} \\ M_{21} \end{bmatrix} = \begin{bmatrix} m_2\ddot{x}_{G2} \\ m_2\ddot{y}_{G2} + m_2 g \\ I_{G2}\ddot{\theta}_2 \\ m_3\ddot{x}_{G3} \\ m_3\ddot{y}_{G3} + m_3 g \\ I_{G3}\ddot{\theta}_3 \\ m_4\ddot{x}_{G4} \\ m_4\ddot{y}_{G4} + m_4 g \\ I_{G4}\ddot{\theta}_4 \end{bmatrix} \tag{4}$$

Where $\dot{x}_{Gi}$ $\dot{y}_{Gi}$, $\ddot{x}_{Gi}$ and $\ddot{y}_{Gi}$ for i=2, 3, 4 are the x and y directions of mass centers velocities and accelerations of the moving links, respectively. $\dot{\theta}_i$ and $\ddot{\theta}_i$ for i=2, 3, 4 are velocities and accelerations respectively, of the moving links considering the input link, follower and coupler. The value of angular velocity of the input link is constant and it is equal to 300 rpm. The position vectors of the mass centers of the ith link are as follows according to Fig 1:

$$\begin{bmatrix} r_{2x} & r_{2y} \\ r'_{2x} & r'_{2y} \\ r_{3x} & r_{3y} \\ r'_{3x} & r'_{3y} \\ r'_{4x} & r'_{4y} \\ r_{4x} & r_{4y} \end{bmatrix} = \begin{bmatrix} r_2 & 0 & 0 & 0 & 0 & 0 \\ 0 & r'_2 & 0 & 0 & 0 & 0 \\ 0 & 0 & r_3 & 0 & 0 & 0 \\ 0 & 0 & 0 & r'_3 & 0 & 0 \\ 0 & 0 & 0 & 0 & r_4 & 0 \\ 0 & 0 & 0 & 0 & 0 & r'_4 \end{bmatrix} \times \begin{bmatrix} -\cos(\theta_2+\alpha_2) & -\sin(\theta_2+\alpha_2) \\ \cos(\theta_2-\beta_2) & \sin(\theta_2-\beta_2) \\ -\cos(\theta_3+\alpha_3) & -\sin(\theta_3+\alpha_3) \\ \cos(\theta_3-\beta_3) & \sin(\theta_3-\beta_3) \\ \cos(\theta_4-\beta_4) & \sin(\theta_4-\beta_4) \\ -\cos(\theta_4+\alpha_4) & -\sin(\theta_4+\alpha_4) \end{bmatrix} \quad (5)$$

Where β_2, β_3 and β_4 are the angles related to ABG_2, BCG_3 and CDG_4, respectively and their equations are presented in the appendix. r'_2, r'_3 and r'_4 ‘are the third side of triangles whose other two sides are r_2, l_2 and r_3, l_3 and r_4, l_4, respectively.

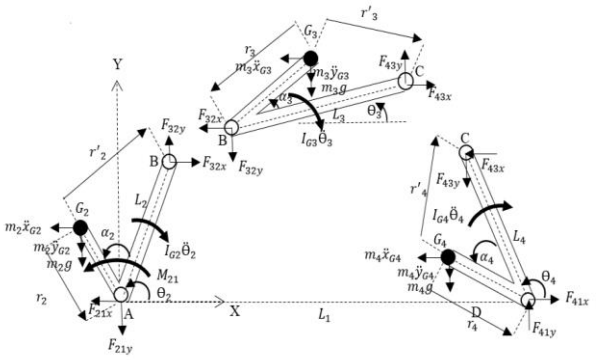

Figure 1. Force Diagram Model of Four-bar Mechanism [26]

3. Multi-objective optimization

Multi-objective optimization or vector optimization was determined to find a vector of design variables while satisfying constraints to give acceptable values of all objective functions.

In terms of multi-objective optimization, the goal is to find the design vector $X^* = \{x_1^*, x_2^*, ..., x_n^*\}^T$ to optimize the objective functions $F = \{f_1(X), f_2(X), ..., f_k(X)\}^T$ under an inequality constraint:

$$g_t(X) \le 0 \qquad t = 1,2,...,m \quad (6)$$

And equality constraints:

$$h_j(X) = 0 \qquad j = 1,2,...,p \quad (7)$$

It is assumed that all objective vectors should be minimized or maximized. This problem is called multi-objective optimization and is categorized as the Pareto approach, as defined below.

3.1. Definition of Pareto dominance

Vector $U = [u_1, u_2, ..., u_n]$ is dominated by the vector $V = [v_1, v_2, ..., v_n]$, if and only if:

$$\forall i \in \{1,2,...,k\}, u_i \le v_i \wedge \exists j \in \{1,2,...,k\} : u_j < v_j \quad (8)$$

3.2. Definition of Pareto Optimality

A point $X^* \in \Omega$, Ω is an acceptable design area that fits equations (9) and (10) and it is Pareto optimal if and only if $F(X^*) \prec F(X)$. In other words:

$$\forall i \in \{1,2,...,k\}, \forall X \in \Omega - \{X^*\} \; f_i(X^*) \le f_j(X) \quad (9)$$

$$\wedge \exists j \in \{1,2,...,k\} : f_j(X^*) < f_j(X) \quad (10)$$

3.3. Definition of Pareto Set

In multi-objective optimization problems, a Pareto collection (P*) contains all optimal Pareto vectors [4, 5].

$$P^* = \{X \in \Omega \mid \exists X' \in \Omega : F(X') \prec F(X)\} \quad (11)$$

One of their uses is to address multi-objective optimization issues since they possess the natural features of evolutionary algorithms and population based or parallel search processes. Thus, the majority of issues and shortcomings related to conventional methods when resolving multi-objective optimization issues are eliminated. As an example, the requirement for numerous runs to determine the Pareto front or quantification of significance of every objective function via numerical weights is eliminated.

4. Differential Evolution Algorithm (DE)

Generally, DE is a random population-based algorithm which is considered to be an evolutionary algorithm [28]. However, it has an inimitable approach for generating new populations. Each population in evolutionary algorithms produces new population using crossover and mutation operators applied to them in sequence. After that, the method of mutation application and its step length is defined considering a random distribution. Nonetheless, in the DE algorithm, first the mutation operator produces a temporary response, followed by the production of a new response using the crossover operator. Furthermore, instead of certain random distribution steps of the mutation, it happens by using the difference between the existing responses from the population.

In the DE algorithm, the step length and direction of mutation are determined by selecting two members of the population randomly and calculating the difference between them. This process is also called the difference vector. Mutation vector is the value of difference vector, and population size is one of the parameters of DE, where the increase in size of the population has a direct effect on the searching capability of the algorithm. Meanwhile, more difference vectors can be found by increasing the population. As a result, the algorithm can search in more directions.

It is better to consider population size of ten times that of the design variables. Increasing size in some cases leads to appropriate results. The weighting factor is another DE parameter that must be small enough so that the algorithm can precisely explore the space. On the other hand, it must be large enough so that the variety of responses could stay at an excellent level. If the population size increases, the weighting parameter must be reduced since there is no need to consider a high size for steps. In this regard, you can refer to experimental results.

Convergence before maturity happens by using higher values for population size and weighting parameters. By increasing the ratio of crossover probability which is considered as one of the parameters of the DE algorithm, we can obtain temporary and new results which lead to a larger set of responses and capacity of searching for the algorithm. The increased probability of crossover in most cases leads to increased convergence speed while reduced crossover probability will result in a robust searching process. Therefore, if the convergence speed decreases, chances of reaching better results will possibly increase.

The algorithm that is used in this study is dynamic differential evolution, where the behavior can randomly change during the

search process [10]. Experimental studies were conducted on a comprehensive set of benchmark functions, including classical problems and shifted large-scale problems. Simulation results demonstrate the efficiency and effectiveness of the proposed heterogeneous DE algorithm. The differential evolution algorithm is used with a randomly selected mutation step between 0.4 and 0.6 and a crossover operator equal to 0.3. The results are obtained by the uniform diversity operator and 500 iterations are used for the optimization process. The optimization parameters have been adopted from ref [12].

5. Multi- Objective Optimization of Four-bar Mechanism

Both the shaking forces and shaking moment must be eliminated in order to obtain complete balancing. However, complete balancing of one leads to unbalancing the other [29]. Engineers can balance the shaking forces by attaching equilibrium weights to the links similar to conventional methods. However, this would increase the mass and moment of inertia of the whole mechanism which leads to increased shaking moment, joint interaction, supported reaction and other mechanism dynamic values. Therefore, the multi-objective optimization method is suggested to address these problems. In order to optimally balance the mechanism, a multi-objective DE algorithm is used. The process was explained in the previous section. The main objective is reducing $[F_{21x}, F_{21y}, F_{41x}, F_{41y}, M_{sh}]$ during the one period of the crank link. In this regard, F_{21x} and F_{21y} represent the horizontal and vertical forces exerted to joints A; F_{41x} and F_{41y} are the horizontal and vertical forces exerted to joint D simultaneously. Joints A and D have been shown in fig. 1. Furthermore, M_{sh} is the moment exerted to the joint of the follower link of the frame. All of these values are equal to:

$$F_{21x} = \sum_{n=1}^{s} \left(F_{21X} \right) \tag{12}$$

$$F_{21y} = \sum_{n=1}^{s} \left(F_{21y} \right) \tag{13}$$

$$F_{41x} = \sum_{n=1}^{s} \left(F_{41X} \right) \tag{14}$$

$$F_{41y} = \sum_{n=1}^{s} \left(F_{41y} \right) \tag{15}$$

$$M_{sh} = \sum_{n=1}^{s} \left(L_1 \sin\theta_1 j \otimes F_{41x} i + L_1 \cos\theta_1 i \otimes F_{41y} j \right) \tag{16}$$

Where S is the number of points for which calculation was conducted during a rotation of the input link, which is considered to be 360 points. Design variables included 16 members as follows:

$$X = \left[L_j \quad \alpha_i \quad m_i \quad I_{Gi} \quad r_2 \quad r_3 \quad r_4 \right] \tag{17}$$

Where L_j indicates the length of the moving links, including, L_2, L_3 and L_4. α_i representing the angle added to θ_i in order to move the mass center of rotating links including α_2 , α_3 and α_4. m_i and I_{Gi} , representing the mass and moment of inertia of the moving links that contain m_2 ، m_3 ، m_4 and I_{G2} ، I_{G3} ، I_{G4} . r_2 ، r_3 ، r_4 are also the relative distances between the center of mass of the links and joint of the related link. The alignment of the mechanisms is in line with the horizon ($\theta_1 = 0$).

$x_{\min}$ and $x_{\max}$ represent the upper and lower limits of design variables. The upper and lower limits for the length of the links are $L_i - 0.1L_i$ and $L_i + 0.1L_i$, respectively. For α_i , 0 and 360 are considered as upper and lower limits. For the other design variables, upper and lower limits are also considered according to the geometry, thickness, length of each link of the original mechanism and the workspace of the mechanism. The range of design variables considered for this optimization problem is presented as; $20 \le r_2 \le 80$ mm, $0.3 \le m_2 \le 4$ kg, $0.0001 \le I_{G2} \le 0.0005\ kg.m^2$, $50 \le r_3 \le 390$ mm, $0.8 \le m_3 \le 5$ kg, $0.05 \le I_{G3} \le 0.15\ kg.m^2$, $40 \le r_4 \le 310$ mm, $0.8 \le m_4 \le 2$ kg, $0.05 \le I_{G4} \le 0.25\ kg.m^2$.

The problem is that the mechanism must be of the Grashof type. The Grashof condition in the four-bar mechanism of the study is in accordance with equation (18).

$$g(x) = L_1 + L_2 \le L_3 + L_4 \tag{18}$$

6. Results and Discussion

In this section, the results of application of the multi-objective differential evolution algorithm presented in the previous section for multi-objective balancing design of a four-bar mechanism model is presented as shown in Fig. 1.

There are ten possible pairs of five objectives that were considered in a five-objective optimization process. A total of 160 choices with a crossover probability of 0.3 and random mutation probability between 0.4 and 0.6 were selected and used in 500 generations. The Pareto fronts of each pair are shown in Figs. 2 and 3.

Obtaining a more favorable value for one objective could possibly result in a worse value for other objectives according to the Figures. The best potential combination of the pair of objectives will be obtained if selection of a set of design variables is made on the basis of the Pareto front.

Hence, if other sets of design variables are chosen, the corresponding values will determine a point which is inferior to the associated Pareto front. This inferior area in the objective functions space for Fig. 2 and Fig. 3 is on the top/right sides. Discovery of an optimal design point is now possible, which is placed on almost all Pareto fronts of Fig. 2 and Fig. 3. Thus, it can be obtained by mapping objective function values of all non-dominated points into 0 and 1 intervals. By utilizing the sum of values for every non-dominated point, design point A is a representation of the minimum of these values. It is evident that design point A is located on approximately all Pareto fronts while every point on the Pareto chart is a representation of a potential choice to address the issue based on the design criteria. The points on the Pareto chart are not superior compared to each other but four points are presented as the suggested points using letters A, B, C and D.

Points A, B, C and D are design points which depict minimum values for F21x, F21y, F41x, and both F41y and Msh, respectively. Moreover, point A is the most important point among other ones. In fact, it is the trade-off point of the Pareto chart. The described mapping method is used in order to find the compromise point.

The points E, F and G are shown in Fig. 2 and Fig.3 and are optimized mechanisms suggested by reference [26] considering three different optimization cases with three types of weight factors. Moreover, point H is the original non-optimized mechanism of reference [26].

The corresponding values of design variables of these selected points, suggested points of reference [26], the original mechanism of reference [26] and the magnitudes of their objective-functions are respectively presented in the table 1 and table 2.

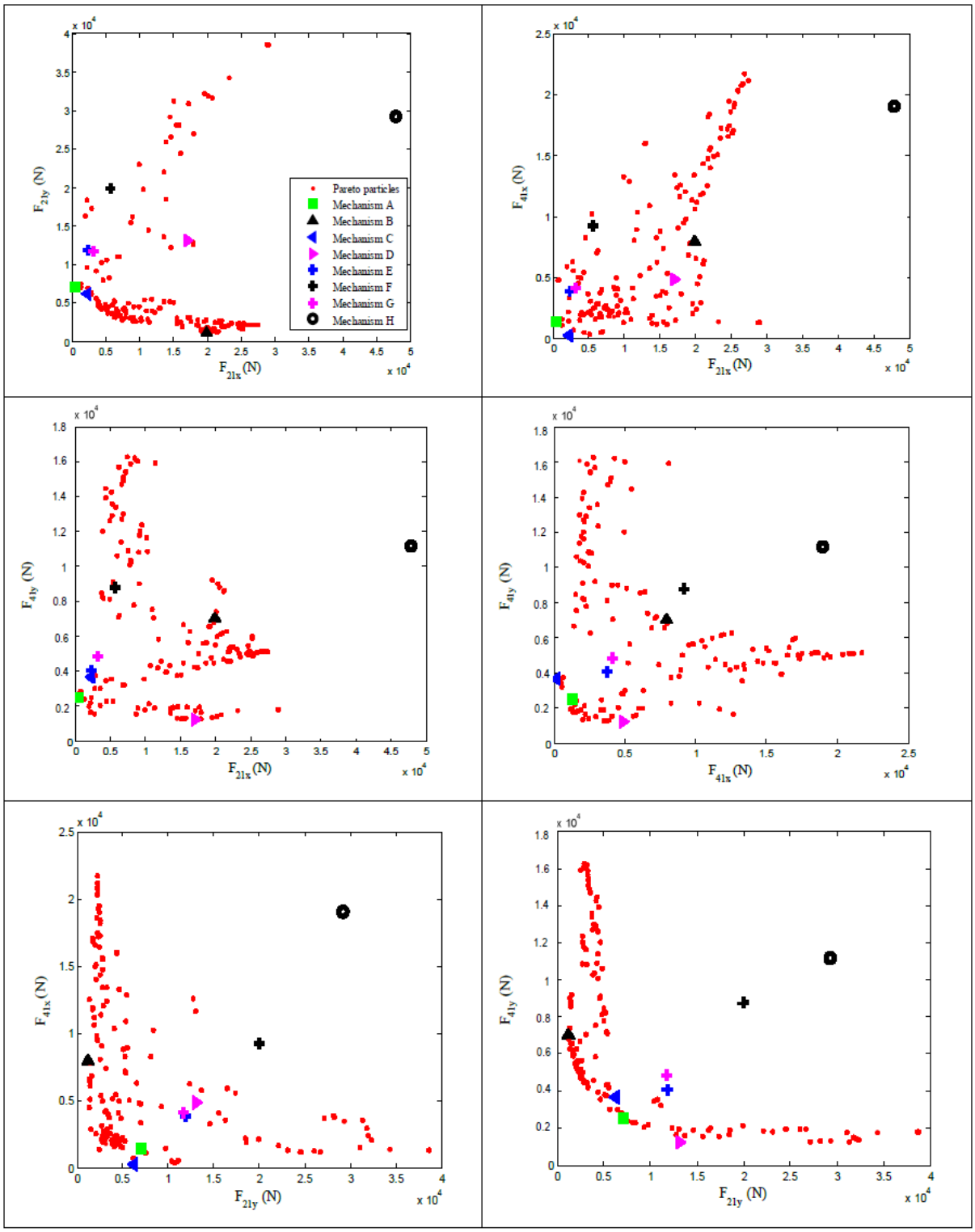

Figure 2. Pareto Fronts of Five-objective Optimization (including shaking forces alone)

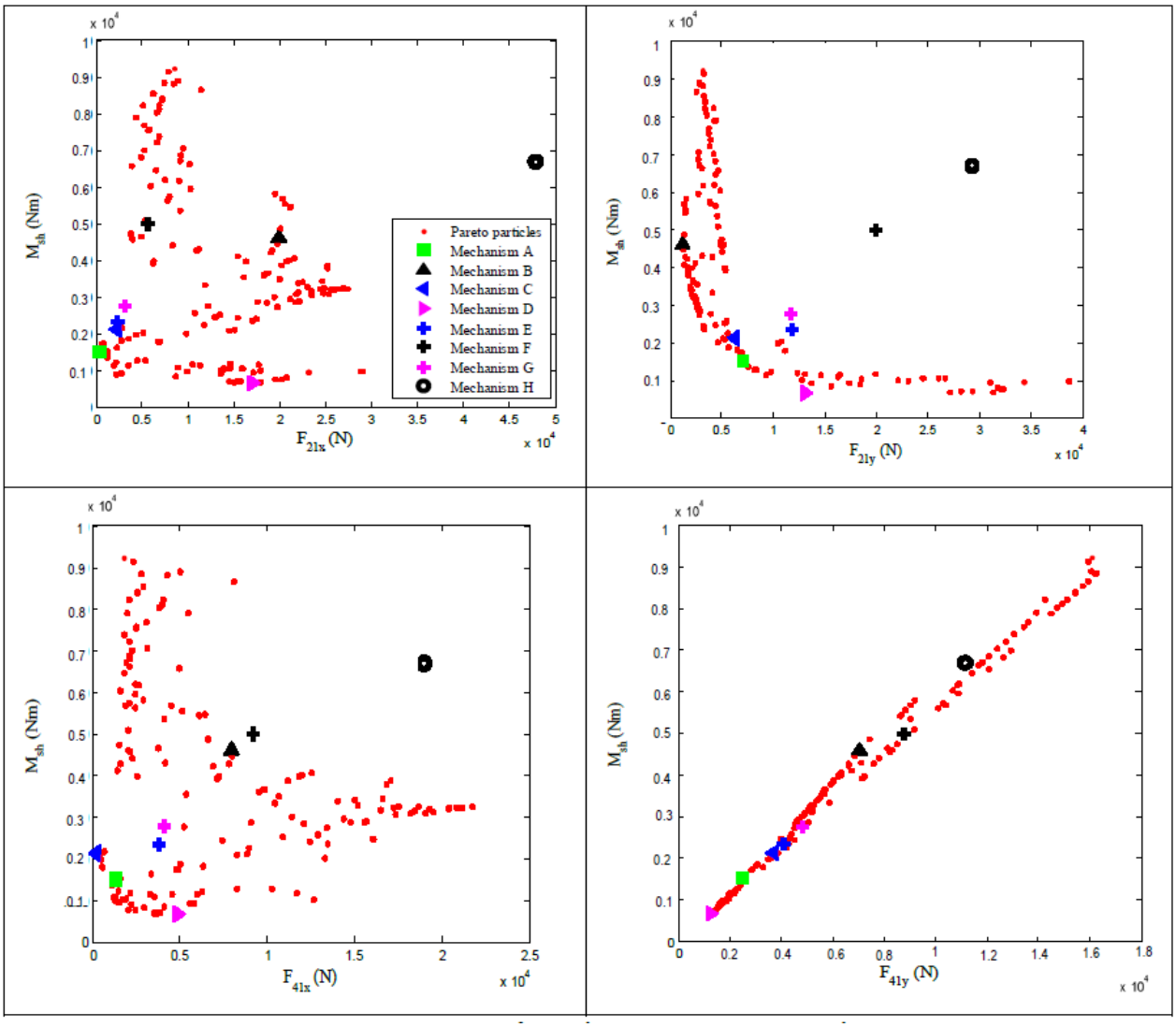

Figure 3. Pareto Fronts of Five-objective Optimization (including shaking moments)

A comparison of the objective function values corresponding to optimum design points A, B, C and D are obtained from optimization of five-objective functions. Comparison of the results obtained for point A in particular with those suggested by reference [26], demonstrates the superiority of the method presented in this study. Thus, these multi-objective optimization shaking moment balancing and shaking forces of planar mechanisms present optimal alternatives of design variables on the basis of Pareto non-dominated points.

Simulation results of force and moment characteristics for points A and the original mechanism are presented in Figure 4. It is clear that simulation results at the suggested point were superior to that of the original mechanism. The red curves in Fig.4 are those drawn with the simulation of this study for the original mechanism of ref [24]. They match the related curves in ref [26]. Therefore, the necessary validation was carried out according to Figure 4 in the paper.

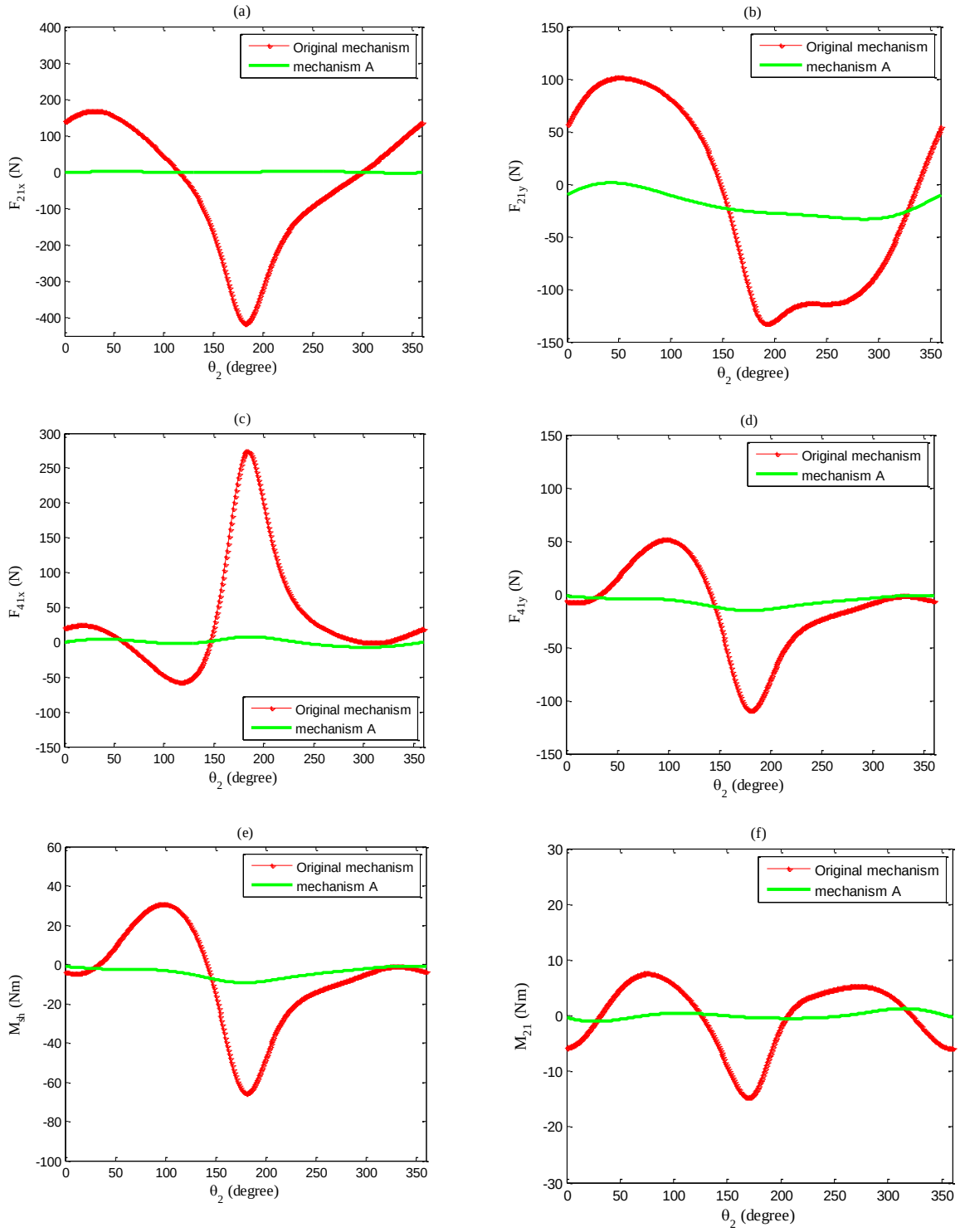

Figure 4. Original mechanism and the suggested values of joint forces for point A (a) and (b) Crank-frame Joint, (c) and (d) Follower-frame Joint, (e) Shaking Moment, (f) Driving Torque

Table 1. Values of design variables of optimal points and reference [18].

No	Design Variables	A	B	C	D	E	F	G	H
1	L_1 *(mm)*	608.1	654.3	575.3	542	570	570	570.2	600
2	L_2 (mm)	90.9	90	90.1	90	95	95	95	100
3	r_2 (mm)	78.1	76.41	79.8	76	66.7	66.7	72.54	50
4	m_2(kg)	0.9886	0.4685	1.0765	1.7652	2.027	3.47	1.755	0.36
5	I_{G2} (kgm^2)	0.0008	0.0045	0.0081	0.0056	42.3×10^{-4}	98.28×10^{-4}	48.93×10^{-4}	4.13×10^{-4}
6	α_2 (Radian)	3.0891	3.7577	3.1329	3.5109	3.0332	3.065	3.032	0
7	L_3 (mm)	430.9	434.5	436.4	437.2	420	420	420	400
8	r_3(mm)	52.3	273.7	64.7	94	77.5	88.73	87.96	200
9	m_3(kg)	0.8926	0.8037	0.8824	1.4484	1.264	2.06	1.23	1.296
10	I_{G3} (kgm^2)	0.0125	0.0170	0.0158	0.0061	4.87×10^{-2}	9.96×10^{-2}	4.43×10^{-2}	1.87×10^{-2}
11	α_3 (Radian)	1.2298	6.0737	6.0086	1.3622	0.1275	0.417	0.1619	0
12	L_4(mm)	351.7	330	351.9	350.6	329.8	313.9	330	320
13	r_4 (mm)	65.3	181.4	59.8	240.3	100.4	128	97	160
14	m_4 (kg)	0.8075	0.8005	0.8540	0.8052	0.866	1.425	1.22	1.046
15	I_{G4} (kgm^2)	0.0051	0.0050	0.0099	0.0053	14.3×10^{-3}	16×10^{-3}	15×10^{-3}	9.85×10^{-3}
16	α_4 (Radian)	0.7607	3.9409	4.9624	1.0595	0.0002	0.0013	0.0023	0

Table 2. Values of objective functions for optimal points and reference [18].

NO	Objective functions	A	B	C	D	E	F	G	H
1	F_{21x}	406.8	19910	2170.6	16968	2312	5678	3158	4706
2	F_{21y}	7054.7	1191	6251.9	13152	11854	19984	11696	29140
3	F_{41x}	1354.1	7969	205.6	4856	3812	9221	4118	18945
4	F_{41y}	2486.4	7032	3682.1	1245	4086	8757	4839	11122
5	Msh	1512	4601	2118.3	675	2329	4991	2759	6673

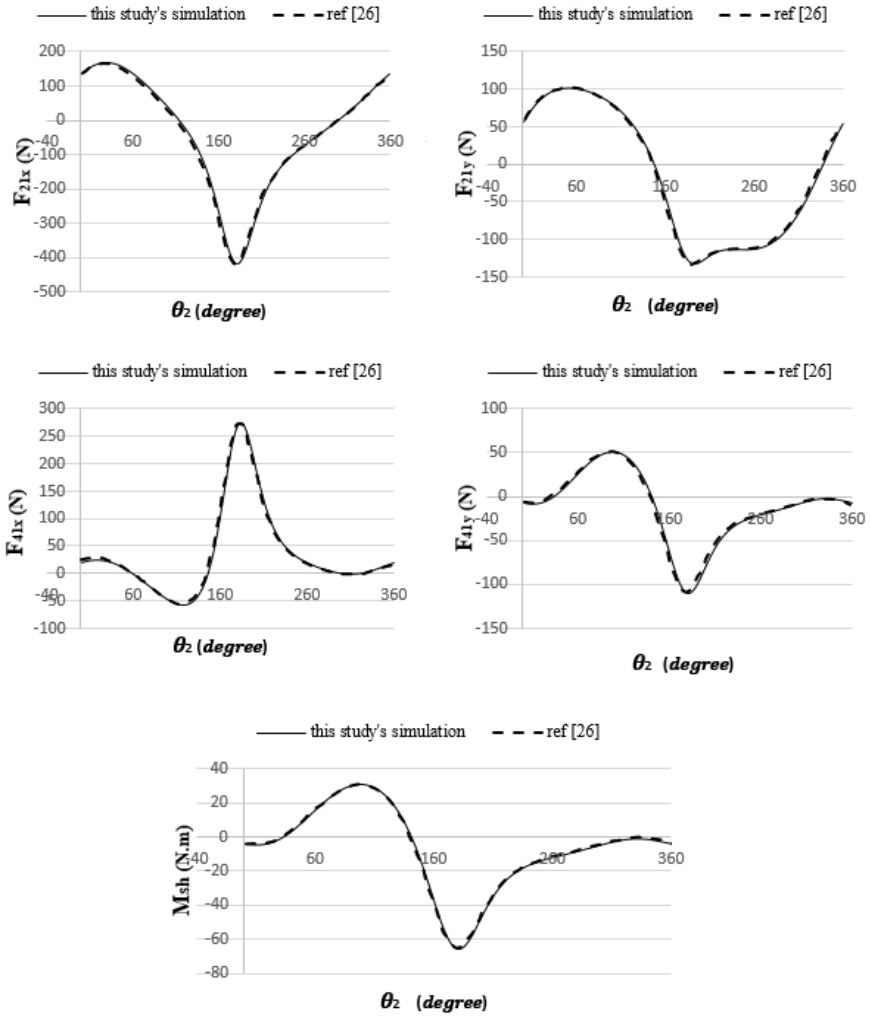

Figure 5. Diagrams of shaking forces and shaking moment for the original mechanism for this simulation and ref [26]

However, the objective function curves for the main mechanism have been plotted in one graph for more clarity, using chart data of Fig. 4 in ref [26], as well as the simulation method of this research. The charts show that a high degree of agreement exists between the two simulations of Ref [26] and this paper. The matching diagrams of the two simulations are shown in Fig. 5 in order to validate the method proposed in this study.

As a natural result of multi-objective optimization, shaking force and shaking moment at the suggested mechanisms A and C of the present article were closer to zero, compared to the original mechanism and optimized mechanisms suggested by reference [26].

Point A and C showed appropriate decrease ratios for all five objective-functions relative to the original mechanism and optimized mechanisms suggested by reference [26] as shown in Tables 3 and 5. During the only crank link period, the maximum shaking force values for the y and x directions and the shaking moment decreased by the ratios given in Tables 3-6, respectively. The decrease ratios of points A and C were better, compared to other studies [26].

Table 3. Decreasing Ratios for Point A Relative to Points E, F, G and H

Objective Functions	Decreasing Ratio for Point A Relative to G	Decreasing Ratio for Point A Relative to F	Decreasing Ratio for Point A Relative to E	Decreasing Ratio for Point A Relative to H
F_{21x}	92.84	87.12	82.41	99.15
F_{21y}	64.68	39.65	40.46	75.86
F_{41x}	85.27	67.01	64.37	92.85
F_{41y}	71.60	48.62	39.15	77.70
M_{sh}	69.71	45.20	35.08	77.40

Table 4. Decreasing Ratios for Point B Relative to Points E, F, G and H

Objective Functions	Decreasing Ratio for Point B Relative to G	Decreasing Ratio for Point B Relative to F	Decreasing Ratio for Point B Relative to E	Decreasing Ratio for Point B Relative to H
F_{21x}	-250.71	-530.5	-761.30	58.47
F_{21y}	94.04	89.81	89.94	95.92
F_{41x}	13.55	-93.55	-109.09	58.03
F_{41y}	19.71	-45.26	-72.04	36.96
M_{sh}	7.85	-66.67	-97.47	31.26

Table 5. Decreasing Ratios for Point C Relative to Points E, F, G and H

Objective Functions	Decreasing Ratio for Point C Relative to G	Decreasing Ratio for Point C Relative to F	Decreasing Ratio for Point C Relative to E	Decreasing Ratio for Point C Relative to H
F_{21x}	61.76	31.25	7.01	95.47
F_{21y}	68.74	46.54	47.26	78.62
F_{41x}	97.77	95.02	94.62	98.92
F_{41y}	57.95	23.92	9.90	66.98
M_{sh}	57.56	23.24	9.05	68.34

Table 6. Decreasing Ratios for Point D Relative to Points E, F, G and H

Objective Functions	Decreasing Ratio for Point D Relative to G	Decreasing Ratio for Point D Relative to F	Decreasing Ratio for Point D Relative to E	Decreasing Ratio for Point D Relative to H
F_{21x}	-199.63	-438.66	-635.84	64.52
F_{21y}	34.45	-11.99	-10.50	55.20
F_{41x}	47.29	-18.01	-27.48	74.41
F_{41y}	85.78	74.28	69.54	88.84
M_{sh}	86.49	75.55	71.04	89.92

On the other hand, a maximum input torque M_{21} = 14.7237 Nm is required to supply a speed of 300 rpm in the main mechanism. An engine with a nominal value of 462.75 watts is required to create this torque as indicated by Equation 19, where P indicates power consumption.

However, the maximum input torque in the trade off point of this study is 1.2715 (N.m) which requires an engine that produces only 40 watts of rated power. This can save 91.36% on power consumption, which would save around 1,500 KJ per hour. Remarkably, this result was obtained although the input torque was not one of the objective functions of this problem. Section f of Fig. 4 also confirms the conclusion that there is a significant decrease in the input torque of the mechanism.

$$P = M_{21} \times \dot{\theta}_2 \tag{19}$$

7. Conclusion

The objective of this research study is to reduce shaking moment and shaking forces at the planar mechanism to address the optimization issue. Using the optimally balanced mechanism improved performance of the mechanism, reduced noise and vibration, and ultimately increased the fatigue life of the mechanism. Contrary to the similar studies in the literature, the sub-components of shaking force and shaking moment were separately considered as five objective functions. A theoretical model for studying shaking moment and force was considered with the speed of 300 rpm at the input link to achieve this goal. A multi-objective differential evolution algorithm was used for optimal balancing design of a four-bar mechanism. The objective functions, which are in conflict with each other, are shaking moment and horizontal and vertical shaking forces. The aforementioned four bar mechanism model multi objective optimization may provide design trade-offs among conflicting objective functions that are not otherwise possible. The four bar mechanism model multi objective optimization enables determination of vital trade-offs between such objective functions. The advantage of the acquired optimal design points is presented in comparison with the ones mentioned in the literature. Moreover,

it was proven that there are several alternatives for designers for optimal design in Pareto fronts. This method can also be used for other spatial and planar mechanisms.

Appendix

Angular positions of coupler and follower links in Equations (1-2) are determined as follows:

$$\theta_3 = 2\tan^{-1}\left(\frac{\mathrm{A}\pm\sqrt{A^2+B^2-C^2}}{\mathrm{B+C}}\right) \quad \text{(A1)}$$

$$\theta_4 = \cos^{-1}\left[\frac{1}{L_4}\left(L_2\cos\theta_2 + L_3\cos\theta_3 - L_1\cos\theta_1\right)\right] \quad \text{(A2)}$$

Where A, B and C are given as:

$$A = -2L_3\left(L_2\sin\theta_2 - L_1\sin\theta_1\right) \quad \text{(A3)}$$

$$B = 2L_3L_1\cos\theta_1 - 2L_2L_3\cos\theta_2 \quad \text{(A4)}$$

$$C = {L_1}^2 + {L_2}^2 + {L_3}^2 - {L_4}^2 - 2L_2L_1\cos\left(\theta_2-\theta_1\right) \quad \text{(A5)}$$

β_2, β_3 and β_3 angles in Eq. (5) are defined as:

$$\beta_2 = \cos^{-1}\left(\frac{\overline{BG_2}^2 + L_2^2 - \overline{AG_2}^2}{2\overline{BG_2}\,L_2}\right) \quad \text{(A6)}$$

$$\beta_3 = \cos^{-1}\left(\frac{\overline{CG_3}^2 + L_3^2 - \overline{BG_3}^2}{2\overline{CG_3}\,L_3}\right) \quad \text{(A7)}$$

$$\beta_4 = \cos^{-1}\left(\frac{\overline{CG_4}^2 + L_4^2 - \overline{DG_4}^2}{2\overline{CG_4}\,L_4}\right) \quad \text{(A8)}$$

$\acute{r}_2$, $\acute{r}_3$ and $\acute{r}_4$ angles in Eq. (5) are defined as:

$$r_2' = \left(\overline{AG_2}^2 + L_2^2 - 2\overline{AG_2}.L_2\cos\alpha_2\right)^{1/2} \quad \text{(A9)}$$

$$r_3' = \left(\overline{BG_3}^2 + L_3^2 - 2\overline{BG_3}.L_3\cos\alpha_3\right)^{1/2} \quad \text{(A10)}$$

$$r_4' = \left(\overline{CG_4}^2 + L_4^2 - 2\overline{CG_4}.L_4\cos\alpha_4\right)^{1/2} \quad \text{(A11)}$$

List of Abbreviation

DE Differential Evolution
GA Genetic Algorithm

References

[1] S. S. Rao, 2009, *Engineering optimization: theory and practice*, John Wiley & Sons,

[2] A. Moradi, A. M. Nafchi, A. Ghanbarzadeh, E. Soodmand, Optimization of linear and nonlinear full vehicle model for improving ride comfort vs. road holding with the Bees Algorithm, in *Proceeding of*, IEEE, pp. 17-22.

[3] A. Moradi, K. H. Shirazi, M. Keshavarz, A. D. Falehi, M. Moradi, Smart piezoelectric patch in non-linear beam: design, vibration control and optimal location, *Transactions of the Institute of Measurement and Control*, Vol. 36, No. 1, pp. 131-144, 2014.

[4] C. A. C. Coello, G. B. Lamont, D. A. Van Veldhuizen, 2007, *Evolutionary algorithms for solving multi-objective problems*, Springer,

[5] M. E. Felezi, S. Vahabi, N. Nariman-Zadeh, Pareto optimal design of reconfigurable rice seedling transplanting mechanisms using multi-objective genetic algorithm, *Neural Computing and Applications*, Vol. 27, No. 7, pp. 1907-1916, 2016.

[6] M. Salehpour, G. Etesami, A. Jamali, N. Nariman-zadeh, Improving ride and handling of vehicle vibration model using Pareto robust genetic algorithms, in *Proceeding of*, IEEE, pp. 272-276.

[7] A. Moradi, H. Makvandi, I. B. Salehpoor, Multi objective optimization of the vibration analysis of composite natural gas pipelines in nonlinear thermal and humidity environment under non-uniform magnetic field, *JOURNAL OF COMPUTATIONAL APPLIED MECHANICS*, Vol. 48, No. 1, pp. 53-64, 2017.

[8] B. C. Arnold, 2015, *Pareto distributions*, Chapman and Hall/CRC,

[9] R. Storn, K. Price, Differential evolution–a simple and efficient heuristic for global optimization over continuous spaces, *Journal of global optimization*, Vol. 11, No. 4, pp. 341-359, 1997.

[10] H. Wang, W. Wang, Z. Cui, H. Sun, S. Rahnamayan, Heterogeneous differential evolution for numerical optimization, *The Scientific World Journal*, Vol. 2014, 2014.

[11] J. Tvrdık, Competitive differential evolution and genetic algorithm in GA-DS toolbox, *Tech. Comput. Prague, Praha, Humusoft*, Vol. 1, No. 2, pp. 99-106, 2006.

[12] G. Etesami, M. E. Felezi, N. Nariman-Zadeh, Pareto Optimal Multi-Objective Dynamical Balancing of a Slider-Crank Mechanism Using Differential Evolution Algorithm, *The International Journal of Automotive Engineering*, Vol. 9, No. 3, pp. 3021-3032, 2019.

[13] F. Qiao, H. Miao, Optimization design for planar four-bar mechanism based on differential evolution, in *Proceeding of*.

[14] R. R. Bulatović, S. R. Dordević, On the optimum synthesis of a four-bar linkage using differential evolution and method of variable controlled deviations, *Mechanism and Machine Theory*, Vol. 44, No. 1, pp. 235-246, 2009.

[15] W. Lin, K. Hsiao, A new differential evolution algorithm with a combined mutation strategy for optimum synthesis of path-generating four-bar mechanisms, *Proceedings of the Institution of Mechanical Engineers, Part C: Journal of*

Mechanical Engineering Science, Vol. 231, No. 14, pp. 2690-2705, 2017.

[16] M. G. Villarreal-Cervantes, C. A. Cruz-Villar, J. Alvarez-Gallegos, E. A. Portilla-Flores, Differential evolution techniques for the structure-control design of a five-bar parallel robot, *Engineering Optimization*, Vol. 42, No. 6, pp. 535-565, 2010.

[17] P. Shiakolas, D. Koladiya, J. Kebrle, On the optimum synthesis of six-bar linkages using differential evolution and the geometric centroid of precision positions technique, *Mechanism and Machine Theory*, Vol. 40, No. 3, pp. 319-335, 2005.

[18] B. Feng, N. Morita, T. Torii, A new optimization method for dynamic design of planar linkage with clearances at joints—optimizing the mass distribution of links to reduce the change of joint forces, *Journal of mechanical design*, Vol. 124, No. 1, pp. 68-73, 2002.

[19] Z. Ye, M. Smith, Complete balancing of planar linkages by an equivalence method, *Mechanism and Machine Theory*, Vol. 29, No. 5, pp. 701-712, 1994.

[20] Z. Li, Sensitivity and robustness of mechanism balancing, *Mechanism and Machine Theory*, Vol. 33, No. 7, pp. 1045-1054, 1998.

[21] V. Arakelian, M. Dahan, Partial shaking moment balancing of fully force balanced linkages, *Mechanism and Machine Theory*, Vol. 36, No. 11-12, pp. 1241-1252, 2001.

[22] V. H. Arakelian, M. Smith, Shaking force and shaking moment balancing of mechanisms: a historical review with new examples, *Journal of Mechanical Design*, Vol. 127, No. 2, pp. 334-339, 2005.

[23] V. Arakelian, Shaking moment cancellation of self-balanced slider–crank mechanical systems by means of optimum mass redistribution, *Mechanics Research Communications*, Vol. 33, No. 6, pp. 846-850, 2006.

[24] F. R. Tepper, G. G. Lowen, General theorems concerning full force balancing of planar linkages by internal mass redistribution, *Journal of Engineering for Industry*, Vol. 94, No. 3, pp. 789-796, 1972.

[25] I. Esat, H. Bahai, A theory of complete force and moment balancing of planer linkage mechanisms, *Mechanism and Machine Theory*, Vol. 34, No. 6, pp. 903-922, 1999.

[26] S. Erkaya, Investigation of balancing problem for a planar mechanism using genetic algorithm, *Journal of Mechanical Science and Technology*, Vol. 27, No. 7, pp. 2153-2160, 2013.

[27] A. Lilla, M. Khan, P. Barendse, Comparison of differential evolution and genetic algorithm in the design of permanent magnet generators, in *Proceeding of*, IEEE, pp. 266-271.

[28] N. K. Madavan, B. A. Biegel, Multiobjective optimization using a Pareto differential evolution approach, 2002.

[29] K. Chaudhary, H. Chaudhary, Optimum Balancing of Slider-crank Mechanism Using Equimomental System of Point-masses, *Procedia Technology*, Vol. 14, pp. 35–42, 12/31, 2014.